Available online at www.sciencedirect.com
SCIENCE DIRECT
Thermochimica Acta 442 (2006) 52–60
thermochimica acta
www.elsevier.com/locate/tca

Method of rapid (100 000 K s^{-1}) controlled cooling and heating of thin samples

Mikhail Merzlyakov *

Materials Science and Engineering Department, Johns Hopkins University, 102 Maryland Hall/3400 N. Charles Street, Baltimore, MD 21218, USA

Available online 9 December 2005

Abstract

A method of rapid controlled cooling and heating of thin samples is developed. The apparatus comprises of a thin-film resistor embedded in a membrane and a sample placed on it, a narrow gap between the membrane and a heat sink, and a control circuit. The resistor acts both as a heater and as a temperature sensor to reduce time constant of the control circuit. The gap between the membrane and the heat sink is filled with gas (e.g., N_2 or He) acting as cooling medium with low thermal inertia. The control circuit applies given rate of temperature changes and measures the power, released on the heater, to determine sample thermal properties such as heat capacity, exothermal/endothermal heat flow, etc. The method allows realizing fast (100 000 K s^{-1}) controlled (e.g., linear) cooling and heating rates regardless of thermal events in a sample, and fast (∼10 μs) switching between ramps and isotherms. Beside calorimetry, the method can be used in a variety of applications, requiring rapid controlled temperature changes of a sample, and in studying of fast thermal processes.

Keywords: Fast temperature control; Fast thermal analysis; Fast scanning calorimetry; Nanocalorimetry; Thin-film calorimetry

1. Introduction

Fast instruments with high cooling and heating rates become more and more important for calorimetry [1–3]. One can find in literature examples of extremely high heating and cooling rates experiments: heating rates up to 10^7 K s^{-1} can be achieved by, e.g. Joule heating of metal wires [4] and up to 10^6 K s^{-1} on thin conductive films [5–7]; cooling rates up to 10^6 K s^{-1} and higher were realized by trapping molten Si droplets between two cryogenically cooled metal anvils [8] or by spattering water mist against cryogenically cooled metal plate [9]. Recently developed scanning microcalorimetry at high cooling rate allows cooling and heating rates up to 10^4 K s^{-1} [10,11]. For quantitative thermal analysis, however, high scanning rate alone is not enough. It is very important to control actively the scanning rate of the sample so that thermal history would not depend on the amount of sample loaded to the measuring system. Without such control any changes in scanning rate due to varying thermal response of a sample would alter crystallization or melting as well as reorganization processes. A 'continuous measuring method' [1], in which a single measuring run covers the entire temperature range of interest, imposes high demands on the stability and reproducibility of temperature program. Therefore fast and active (in real time) control over the sample temperature is the key for a successful method. The aim of the present study is to test a plausibility of a new method of rapid controlled cooling and heating of thin samples, which can serve as a core for a variety of fast thermal analysis instruments.

2. Measuring approach

2.1. Sample size

In order to follow rapid temperature changes the sample must be small, at least in one dimension. Length of thermal waves propagation in a time scale τ is given as $l = (\kappa\tau/\pi\rho c_p)^{1/2}$, where κ, ρ and c_p are thermal conductivity, density and specific heat capacity of the material, respectively. The time scale for rapid scanning experiments is very short, e.g. τ = 1 ms when one wants to scan at 1000 K s^{-1} with 1 K resolution. For typical polymers at τ = 1 ms $l \sim 5$ μm. In this example making the polymer sample thicker than 5 μm would create temperature gradient across the sample larger than 1 K at 1000 K s^{-1}. Higher scanning rates, i.e. shorter τ, would result even in larger gradient. Thermal

* Tel.: +1 410 516 7142; fax: +1 410 516 5293.
E-mail address: mikhail.merzliakov@jhu.edu.

0040-6031/$ – see front matter © 2005 Elsevier B.V. All rights reserved.
doi:10.1016/j.tca.2005.11.018

events, like melting, lead to c_p increase (e.g., by a factor of 20 for polycaprolactone) and may further increase temperature gradient within the material, which in turn requires even thinner sample.

2.2. Cooling medium

Good thermal conducting gas and solid have comparable thermal wave lengths (at $\tau = 1$ ms for helium at ambient pressure $l \sim 0.23$ mm, for copper $l \sim 0.19$ mm). Put another way: in gaseous or solid cooling media, temperature waves propagate with comparable rates. However, at the same geometry, a gas cooling medium would require approximately three orders of magnitude lower power to achieve the same temperature distribution. Since the sample should be thin, it would not require a lot of cooling power for rapid cooling anyway. Therefore having a gas instead of a solid as a cooling medium is more attractive since it would require much less power to control the sample temperature, which, in turn, would lead to much better resolution of the sample heat flow.

2.3. Fast temperature control

The majority of existing measuring setups have separate heating and temperature sensing components, see e.g., [12]. (There is also a large group of methods using non-contact principles for heating and/or for temperature sensing, which is not discussed here.) Obvious way to improve time response of calorimetric measuring cells or hot stages is to scale down the existing layouts, which also greatly increases sensitivity of the instruments. Nowadays that can be done to the large extend using lithographic technique [13–18]. This downsizing indeed improves thermal coupling between the heater and the temperature sensor, but at the same time, it increases parasitic electrical coupling between them. Even when heating and temperature sensing components made electrically insolated, capacitive and inductive coupling is inevitable and become very pronounce at a small scale, especially at short time intervals (see example of that below, Fig. 5b). Therefore two-component setup for fast temperature control has inherent limitation in speed and accuracy. A possible solution is a use of one-component setup, where the same electrical component, a resistor, acts as a heater and as a temperature sensor.

The idea to use heating element as a thermometer is not new, though. There are some methods described in literature, which use a heater as a thermometer. As for temperature sensing applications, for example, specific heat spectroscopy [19] and 3 omega method [20] are well-known techniques that use a thin-film heater as a temperature sensor for heat capacity and thermal conductivity measurements of a sample placed on the heater-thermometer. Measurements are performed by applying oscillating power to the heater-thermometer and by measuring amplitude of third harmonic of oscillating voltage on the heater-thermometer, which is proportional to the temperature oscillations. However there is no active control of the sample temperature. As the heater is deposited on thick substrate (infinite thick for temperature waves at frequencies of interest) and sample used is thick (also infinite thick for the temperature waves), the sample temperature oscillations are much smaller than they could be in case of thin-film sample and thin-film substrate, limiting the sensitivity and upper frequency range. Some researchers used 3 omega method to measure thermal conductivity of thin films [21] but still with a bulky thick substrate having the same limitations.

As for temperature control applications, Heap and coworkers described a method that uses the resistance of electrolyte to control its temperature [22]. However this method is relatively slow (heating and cooling rates up to 20 K s^{-1}), and does not suitable for heat flow measurements; controlled power to the heater is applied only during isothermal mode of operation; cooling and heating are uncontrolled (free cooling is assisted by forced cold air whereas maximum heating power is applied during heating).

Buzin et al. reported a way to measure power and temperature of Wollaston wire probe for scanning thermal microscopy [23]. The method allows simultaneous and direct measurement of both power and temperature of the probe.

Fast scanning rate microcalorimeter [5–7] uses a thin-film heater as a temperature sensor for heat capacity measurements during scanning of temperature. The heater is deposited on thin-film substrate. Known amount of power, usually determined by constant electric current, is applied to the heater and a temperature rise of the heater is measured as a function of time. However different amount of the same material results in different rate of temperature increase and, therefore, in different thermal history, which complicates the analysis. In addition, only experiments on heating are possible because the substrate is placed in vacuum. (The membrane passively cools at a rate of 1–2 K ms^{-1} [6], but no measurements are performed on cooling).

2.4. Control circuit

There are several possible ways to use a resistive element simultaneously as a heater and as a temperature sensor. One way is to connect the resistor periodically for a short time to the heater circuit and to the thermometer circuit, using a fast switch, such as field-effect transistor (FET) operating at MHz frequency. Another possibility is to use an analog divider to calculate in real time the resistance of the heater at any non-zero current through it; providing large temperature coefficient of resistance (TCR) this resistance signal would represent temperature of the heater. Existing analog dividers have good accuracy (better than 0.1%) and operate at frequencies up to 10 MHz and higher [24]. Utilizing digital divider at that speed will require very fast analog-to-digital and digital-to-analog converters and will lead to unnecessary circuit complication (ADC → numeric processor → DAC). However in near future digital divider might be the circuit of choice with advantages in flexibility and accuracy.

Block diagram of a control circuit with analog divider is shown in Fig. 1. The output of differential amplifiers A_2 and A_3 equals to the voltage drops $U_{R_{ref}}$ and U_{R_h} on reference resistor R_{ref} and on heater-thermometer resistor R_h, respectively. Analog

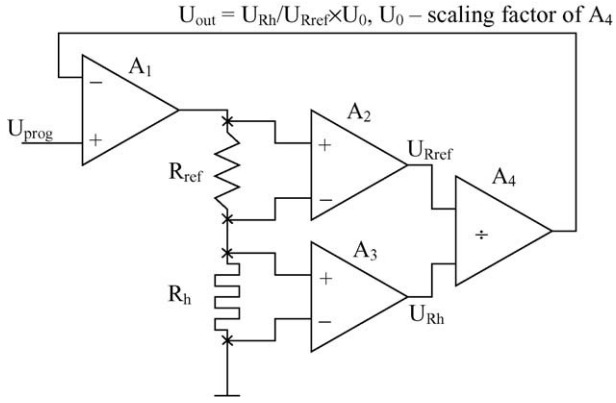

Fig. 1. Block diagram of the control circuit.

divider has transfer function

$$U_{\text{out}} = \frac{U_{\text{Rh}}}{U_{R_{\text{ref}}}} \times U_0 \quad (1)$$

where U_0 is a scaling factor. If the heater-thermometer resistor has small geometry (thin film of micrometer thickness or less), relative small current will appreciably affect the temperature of the resistor, and, therefore, its resistance. The reference resistor is chosen intentionally with very low TCR (<2 ppm K^{-1}), i.e. with constant resistance, R_{ref} = constant, in the whole range of currents used. Since both resistors are in series, $U_{R_h}/U_{R_{\text{ref}}} = R_h/R_{\text{ref}}$, and therefore, the resistance of the heater-thermometer R_h is proportional to U_{out}

$$R_h = \frac{R_{\text{ref}}}{U_0} \times U_{\text{out}} \quad (2)$$

Last part of the circuit is the temperature controller A_1. The controller adjusts the current through the resistors to minimize the difference between the U_{prog} and U_{out}. Therefore, the resistance variations of R_h are proportional to U_{prog}. In first approximation, R_h is a linear function of temperature. Thus, the temperature of the heater-thermometer is proportional to U_{prog}. For example, varying U_{prog} linearly with time makes temperature of the heater R_h also varies linearly. Non-linear part of R_h temperature dependence can be easily accounted for by adjusting U_{prog} time profile.

2.5. Measuring cell

An example of the layout of measuring cell is shown in Fig. 2. Sample can be deposited on the membrane on the area, occupied by the heater-thermometer. During operation, rapid heating or cooling of the membrane generates acoustic waves in the gas (repeated temperature scans in milliseconds range with microcalorimeter sensors from Allen's setup [5–7] produced an audible tone). These acoustic waves may induce strain in the membrane and strain-induced resistance changes of the heater-thermometer, which would impair temperature readings. To minimize that effect, the membrane, ideally, should face the heat sink from both sides symmetrically. In addition, strain in the membrane can be induced by thermal stresses (thermal mismatch between the membrane and the supporting frame) and by a sample [25]. This induced strain may alter TCR of the heater which would require careful temperature calibration and interpretation of the resistance data.

2.6. Modes of operation

2.6.1. Isothermal mode

In linear approximation the resistance of the heater-thermometer is proportional to the program temperature: $R_h(T_h) = R_h(T_0) + \alpha(T_h - T_0) = R_{\text{ref}} \times U_{\text{out}}/U_0 \approx R_{\text{ref}} \times U_{\text{prog}}/U_0$, where T_h is the temperature of the heater-thermometer, $T_{h\,\min} < T_0 < T_{h\,\max}$, R_{ref} and U_0 are constant, α is TCR of the heater. If U_{prog} stays constant, then T_h and the sample temperature remain constant regardless of any heat released/absorbed by the sample. The power released on the heater is determined as $P_h = U_{R_h}^2/R_h$, or $P_h \propto U_{R_h} \times U_{R_{\text{ref}}}$, or $P_h \propto U_{R_h}^2/U_{\text{prog}}$.

2.6.2. Temperature scanning mode

If U_{prog} varies linearly with time between $U_{\text{prog}\,\min}$ and $U_{\text{prog}\,\max}$ (a saw-tooth profile), then T_h increases and decreases linearly with time. Assume we have thin-film heater-thermometer placed at some distance from heat sink in gas (e.g., N_2 or He), as shown in Fig. 2. In first approximation a heat leakage via gas P_l equals to $K(T_h - T_s)$, where thermal conductance coefficient K depends on cell geometry, gas type and pressure. The power released on the empty heater P_e depends on scanning rate and is given as $P_e = P_l + C_e \times dT_h/dt$, where C_e is an effective heat capacity of the membrane and of the heater-thermometer (it may also include parameter of the ambient gas) and dT_h/dt is a scanning rate. The power released on the heater loaded with the sample, P_s, is given as $P_s = P_e + C_s \times dT_h/dt$, where C_s is an effective heat capacity of the sample.

As can be seen from equations for P_e and P_s, heat leakage via gas P_l can be determined at very slow scanning

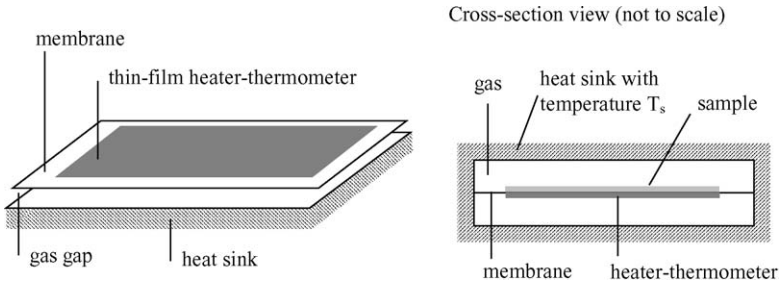

Fig. 2. Example of the layout of measuring cell.

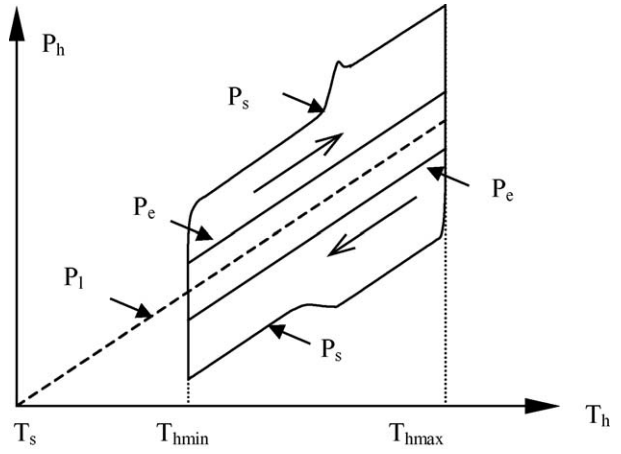

Fig. 3. Power vs. temperature curves (schematic) of empty runs, P_e, and sample runs, P_s. Actual shape of P_e does not scale linearly with temperature, see Fig. 10.

rates, when $dT_h/dt \to 0$. On the other hand, to get higher resolution in C_s, scanning rate should be higher. The limiting factor for cooling rate is that P_s should be positive, in other words, cooling rate $|dT_h/dt|$ should be smaller than $P_l/(C_e + C_s) = K(T_h - T_s)/(C_e + C_s)$. (Actually the value of P_l here should be substituted by $P_l - P_{h\,min}$, where $P_{h\,min}$ is the minimum power, released on the heater. This non-zero value comes from non-zero current through the heater needed for the divider part of the circuit to work properly. In real design, $P_{h\,min}$ can be four to five orders of magnitude lower than the maximum power released by the heater $P_{h\,max}$, so we can neglect $P_{h\,min}$).

The limiting factor for heating rate is $P_{h\,max}$, so that heating rate cannot be higher than $(P_{h\,max} - P_l)/(C_e + C_s) = (P_{h\,max} - K(T_h - T_s))/(C_e + C_s)$. In order for the circuit to avoid "clipping" (reaching the maximum or minimum of the P_h range) the rate of U_{prog} changes with time should stay within the limit determined by dT_h/dt. The value of U_{prog} can vary from $U_{prog\,min} \propto R_h(T_{h\,min})$ to $U_{prog\,max} \propto R_h(T_{h\,max})$. $T_{h\,min}$ should not be very close to T_s to have enough "spare" cooling power, see Fig. 3. The presence of the sample can slightly change the shape of P_l versus T_h (can change the thermal conductance coefficient K), but "new" P_l can be measured directly at $dT_h/dt \to 0$.

2.6.3. Temperature oscillating mode

In oscillating mode U_{prog}, being constant or varying relatively slowly, can be superimposed with small oscillations at some frequency ω with amplitude $A_U \ll U_{prog}$. Heat capacity $C_s + C_e$ at frequency ω is proportional to $i\omega A_U/A_{Ph}$, where A_{Ph} is an oscillating part of P_h. Averaged values (averaged over the oscillating period) of U_{prog} and P_h can be treated the same way as in scanning mode. This operating mode resembles power-compensated TMDSC method, actual scanning rate and amplitude of temperature oscillations are not affected by sample thermal response.

2.6.4. "1 Omega" calorimeter

Simplified circuit for temperature oscillating mode is shown in Fig. 4. The temperature controller is omitted, which allows temperature oscillations at even higher frequencies. In

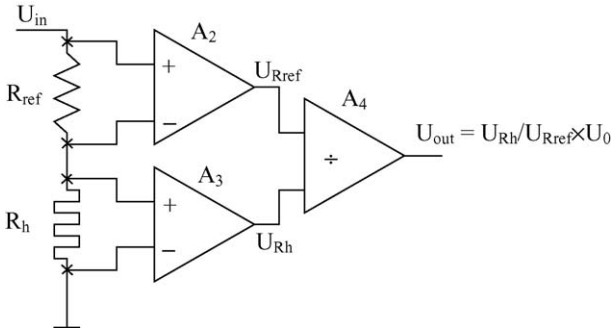

Fig. 4. Block diagram of the simplified circuit for "1 omega" setup.

this setup U_{in} (being constant or varying relatively slowly) is also superimposed with small oscillations with amplitude $A_U \ll U_{in}$ at some frequency ω. Oscillating part of U_{out}, $A_{U_{out}}$ is given as $A_{U_{out}} \propto 2\alpha U_{in} A_U (K - P_h\alpha - i\omega(C_s + C_e))/((K - P_h\alpha)^2 - \omega^2(C_s + C_e))$, where α is TCR of the heater, $C_s + C_e$ is effective heat capacity of the sample and of the membrane with the heater at frequency ω. At high frequencies $A_{U_{out}} \propto i2\alpha U_{in} A_U/(\omega(C_s + C_e))$. This setup has advantage over 3 omega system: it does not require a bridge with adjustable resistors or a differential amplifier with tunable gain to balance out the basic harmonic. In addition the proposed sensor setup has a thin-film substrate and a gas as a cooling media and therefore can work at higher frequencies with lower oscillating power input than 3 omega method.

3. Experimental tests

To prove the plausibility of the proposed setup, two different thin film heaters were used. One is the heater in a vacuum gauge TCG-3880 [26], another is a microcalorimeter sensor from a setup used by Allen and coworkers [5–7]. The control circuit was made on 4-quadrant multiplier/divider AD734 from Analog Devises, USA, connected as a divider with direct denominator control [24]; operational amplifiers AD712 from Analog Devises, USA; and current feedback amplifier LT1210 from Linear Technology, USA, which was used to drive the heater/reference resistor part of the circuit. Reference resistors were Vishay S102K. A function generator was a self-made analog generator. Electrical signals were digitized using 12 bit 25 MHz digital storage oscilloscope ADC-212, Pico Technology, UK. Each curve is an average of approximately 100 scans. No slide averaging was applied to any measured curve.

3.1. Performance of the divider and of the heater-thermometer

Thin silicon nitrate membrane of vacuum gauges surrounded by gas allows achieving easily 40 000 K s^{-1} heating and cooling rates with large temperature swings [27]. For first experiments a thin-film heater of a vacuum gauge TCG-3880 was used as a heater-thermometer because a thermopile on the sensor allows monitoring to some extend temperature of the heater. Fig. 5 shows two voltage traces, U_{in} and U_{out}, during one period of

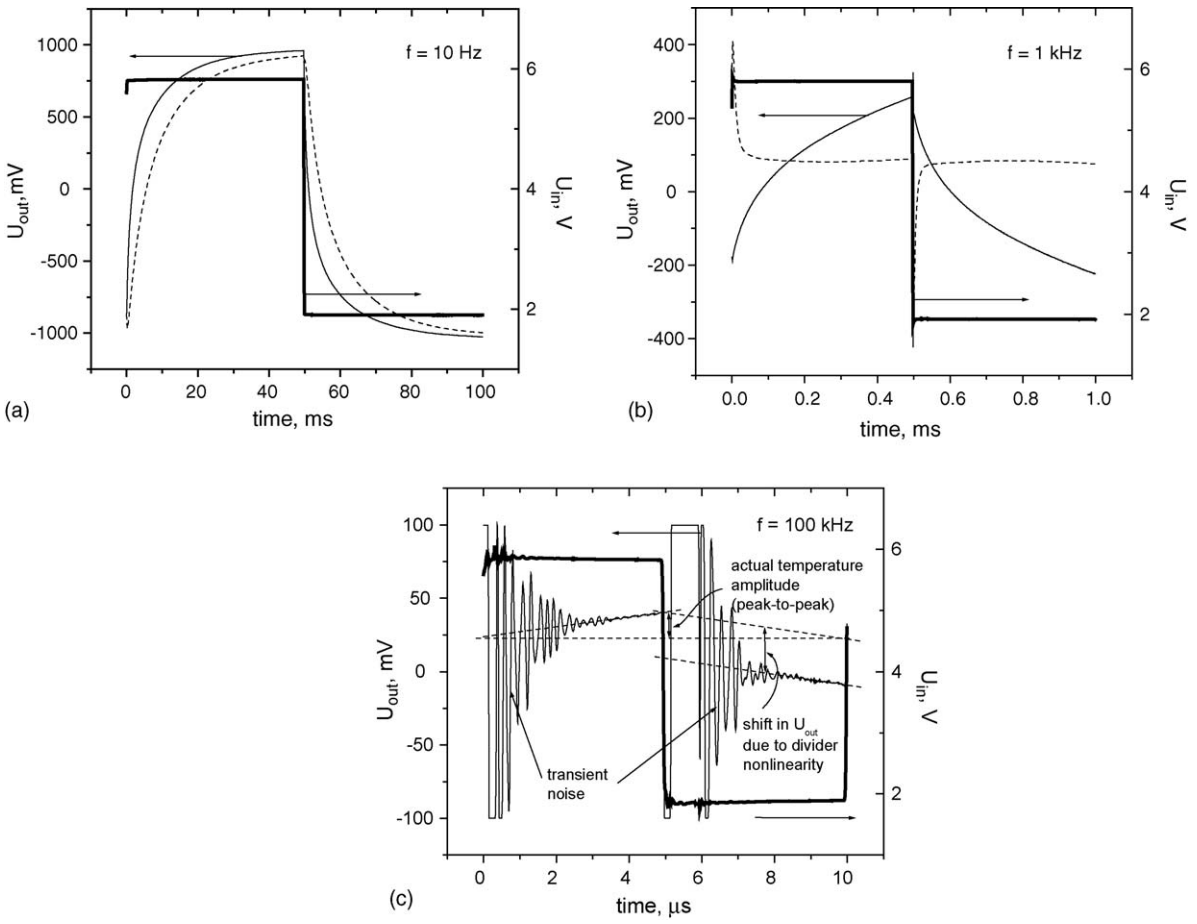

Fig. 5. Input voltage U_{in}, thick lines, and output voltage U_{out}, thin lines, vs. time at different frequencies of U_{in} oscillations. DC component of U_{out}, U_{offset}, was subtracted for clarity. Dotted lines show signal from the thermopile with hot junctions close to the heater. $R_{ref} = 2 \times 374\,\Omega$, $U_0 = 9.9$ V, $U_{offset} = 8.53$ V.

rectangular voltage oscillations of U_{in} for the circuit shown in Fig. 4. The traces of U_{out} in Fig. 5 correspond to temperature changes of the heater-thermometer. Note that for clarity U_{out} is shown without DC component. Dotted lines in Fig. 5a and b shows signal from the thermopile. At the time scale larger than the thermal lag between the heater and the hot junctions (∼5 ms [26]) the thermopile signal can represent the temperature of the membrane closed to the heater, see Fig. 5a. However, at the time scale <5 ms the thermopile ceases to pick up any temperature changes of the heater. Moreover, thermopile output has glitches every time the input voltage U_{in} changes stepwise, Fig. 5b. This is a signature of capacitive coupling between the heater and the thermopile. This parasitic coupling dominates the thermopile output signal and completely misrepresents the temperature of the heater at millisecond time scale. On the contrary, the divider signal at the same conditions represents the temperature of the heater very clearly without artifacts. Glitches in divider signal U_{out} appears only at much shorter time scale, Fig. 5c.

On Fig. 5c transient processes in divider signal U_{out} are settled during 3 μs after step-wise changes in U_{in}. After that one can see clearly how the heater temperature rises and falls, depending on the U_{in}. Part of U_{in} may actually come through the divider to the U_{out} due to non-linearity of the divider or common mode error. This may account for the offset of U_{out} trace at different U_{in}. Actual peak-to-peak amplitude of U_{out} is approximately 18 mV. Time constant of temperature changes is lower than 3 μs. Time constant of temperature measurements can be estimated as 1 μs or even faster under absence of transient noise (e.g. at constant U_{in}). This time constant is a response time when the temperature changes of the heater can be picked up by the divider. It is not the time constant for the whole measuring cell (heater, membrane, heat sink, gas, etc.) to reach steady state at given input power (which is in the order of a few milliseconds as can be judged from Fig. 5a).

Xensor integration specified resistance temperature coefficient of the heater as $0.6\,\Omega\,K^{-1}$ [26]. As reported by Adamovsky et al. [10] R_h of TCG-3880 equals to 475 and 706 Ω at 100 and 500 K, respectively. This results in TCR of $0.5775\,\Omega\,K^{-1}$. The latter value was used for further calculations.

In experiments on Fig. 5 one can estimated the sensitivity of the U_{out} to the resistance changes in R_h using Eq. (2) as $U_0/R_{ref} = 9.9\,V/748\,\Omega \cong 13.2\,mV\,\Omega^{-1}$. Then the sensitivity of the U_{out} to the temperature changes of the heater is $13.2\,mV\,\Omega^{-1}/0.5775\,\Omega\,K^{-1} \cong 7.64\,mV\,K^{-1}$. Then the peak-to-peak temperature amplitude at 100 kHz (Fig. 5c) equals to $18\,mV/7.64\,mV\,K^{-1} \cong 2.36$ K. This corresponds to the heating and cooling rates of $2.36\,K/5\,\mu s \cong 470\,K\,ms^{-1}$ or

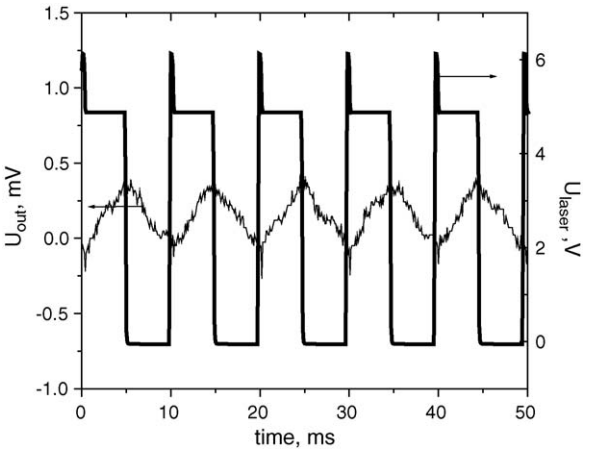

Fig. 6. Voltage changes on laser diode U_{laser}, thick line, and output voltage U_{out}, thin line, vs. time. U_{in} was kept constant. DC component of U_{out} was subtracted for clarity.

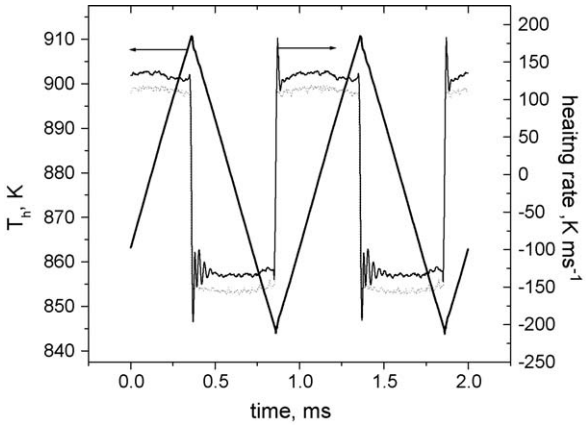

Fig. 8. Temperature of the heater T_h, and heating rate of the heater vs. time. Dotted line shows time derivative of program voltage U_{prog} and is vertically shifted for clarity.

470 000 K s^{-1}. Use of helium instead of nitrogen will allow higher voltage applied to the heater and can easily increase heating and cooling rates four-fold.

Fig. 6 shows the U_{out} on exposing the sensor to a laser diode radiation on frequency of 100 Hz. One can clearly see oscillations of U_{out} with peak-to-peak amplitude ~0.4 mV. This corresponds to peak-to-peak temperature oscillations of 50 mK. The membrane temperature increases or decreases linearly with time, as the laser is turned on or off. The quality of U_{out} allows resolving much smaller amplitudes, approximately two orders of magnitude smaller if one uses selective detection such as a lock-in amplifier. Note that it would require at least 20 bit conversion to achieve similar resolution by A/D converters instead of analog divider.

The heater in TCG-3880 physically allows inducing and measuring temperature oscillations at frequency of 1 MHz and allows monitoring and controlling temperature changes with time constant of approximately 1 μs. Temperature control circuit, discussed in the following section, has additional low-pass filter. This filter slows down the response time of the controller but allows handling transient processes, such as seen during step-wise changes of U_{in} in Fig. 5c.

3.2. Scanning mode

Thermopile of TCG-3880 sensor allows monitoring of heater temperature, providing that rate of U_{prog} changes is low (since thermal lag between hot junctions of the thermopile and the heater is approximately 5 ms). Fig. 7 shows comparisons of the U_{out} and thermopile output voltage U_{tp} at different frequencies of U_{prog} oscillations for the circuit shown in Fig. 1.

The shape of U_{prog} in those experiments was a saw-tooth to realize linear heating and cooling. As one can see, U_{out}, and therefore the temperature of the heater, indeed changes linearly with time. In Fig. 7b one can see how temperature oscillations of the thermopile lag behind of temperature oscillations of the heater.

Another example of linear heating and cooling is shown in Fig. 8. Temperature of the heater T_h, was calculated from U_{out} by Eq. (2) and TCR of the heater. In this experiment heating and cooling rates are constant and equal ~130 000 K s^{-1}. Small

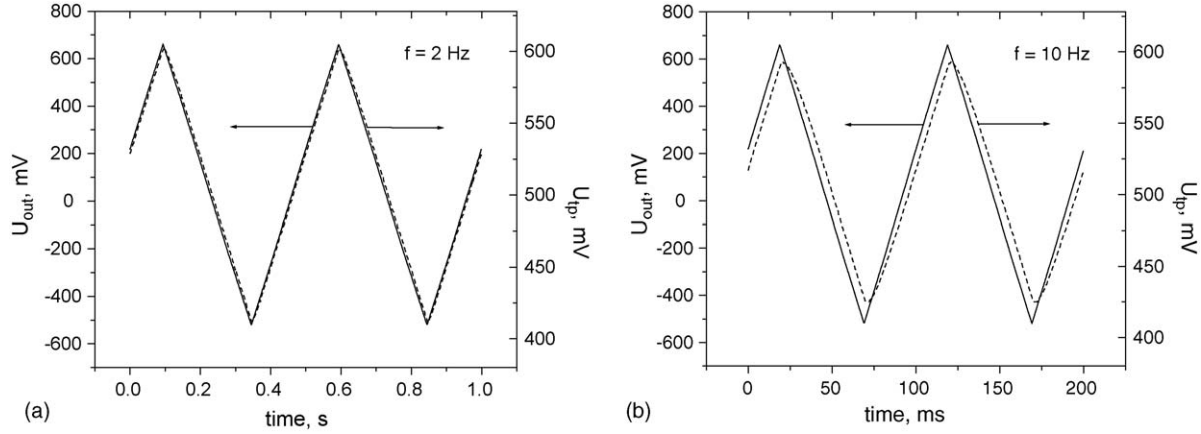

Fig. 7. Comparison of output voltage U_{out}, solid lines, and thermopile voltage U_{tp}, dashed lines vs. time. DC component of U_{out}, U_{offset}, was subtracted for clarity. $R_{ref} = 2 \times 374\,\Omega$, $U_0 = 7.3$ V, $U_{offset} = 8.73$ V.

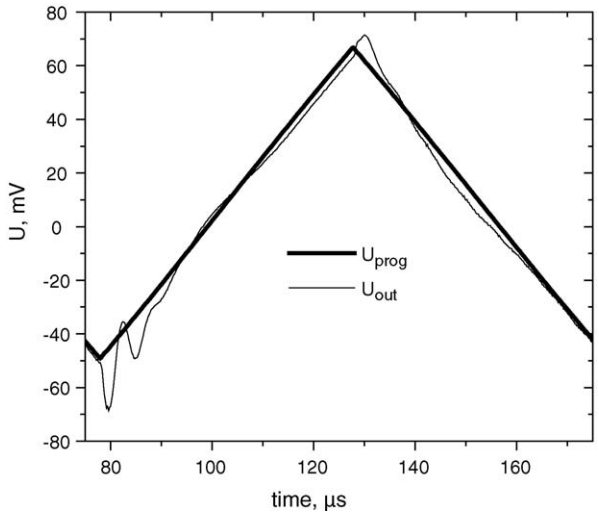

Fig. 9. Program voltage U_{prog}, thick line, and output voltage U_{out}, thin line vs. time. DC component of U_{prog} and U_{out} was subtracted for clarity.

gradual deviations in scanning rate during ramps are due to non-ideal shape of saw-tooth (U_{prog}) in analog function generator, which was used to drive the control circuit (see dotted line in Fig. 8). There are spikes in heating rates at the beginning of each ramp for ~20 μs caused by transient response of the control circuit. In addition, on switching from heating to cooling the spikes are followed by some oscillations for ~100 μs (over first ~10 K of cooling ramps). This instability is due to divider output signal, which degrades as the feedback tries to drive as low current through the heater as possible at the beginning of the cooling ramp. No such instability was observed during switching from cooling to heating.

Fig. 9 gives a closer look at transient processes during switching between linear cooling and heating. Time constant of the temperature controller is approximately 10 μs, setting time is approximately 30 μs.

Fig. 10 shows a power released on the heater P_h versus heater temperature T_h at different scanning rates for an empty membrane (without a sample). This figure is similar to Fig. 3 for power profile of empty membrane P_e. Note that P_e does not scale linearly with temperature and scanning rate, but it depends on the whole temperature-time profile. This is more apparent for TCG-3880 sensor, Fig. 10a, which has a small heating area, compared to the whole membrane. In a short time scale, e.g. at the beginning of heating ramp in 5 ms scan, the heater has to increase the temperature of only a small portion of the membrane near the heater. That is why the heating power is relatively low. Later in the ramp increasingly larger area of the membrane "feels" the temperature increase of the heater, resulting in progressively larger heating power needed to keep up with temperature increase. It is difficult to estimate accurately a particular distribution of thermal waves in the membrane and in the gas and its contribution to the total power. However, since the heater temperature is controlled, temperature waves the heater generates are the same with or without a sample allowing accurate determination of the sample heat flow.

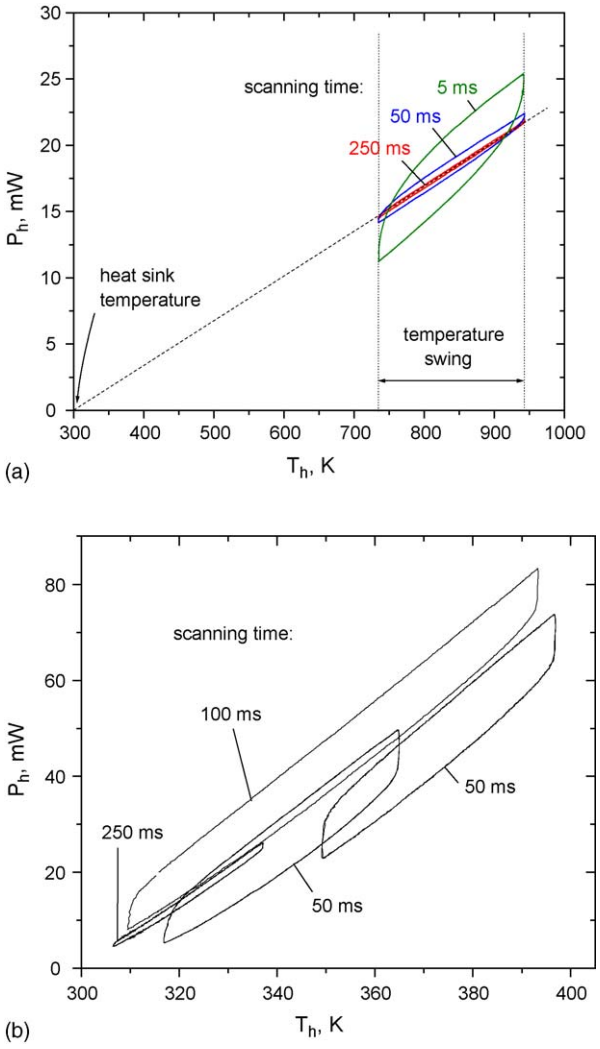

Fig. 10. Power vs. temperature curves of empty heater at different scanning rates in (a) TCG-3880 sensor and (b) microcalorimeter sensor [5–7]. Scanning time means the time for one temperature ramp. Heat sink temperature in the experiments on (b) was slightly dependent on temperature scanning interval.

In experiments on Fig. 10a the resolution of power was approximately 10 μW. At 5 ms scanning time, i.e. at 200 K/5 ms = 40 K ms^{-1} heating and cooling rate, the resolution in heat capacity can be estimated as 10 μW/40 K ms^{-1} = 250 pJ K^{-1}.

Microcalorimeter sensor (Fig. 10b) has much larger heater area and narrower air gap, which leads to larger thermal conductance coefficient ($K \cong 800\ \mu W\ K^{-1}$ for microcalorimeter sensor, $K \cong 30\ \mu W\ K^{-1}$ for TCG-3880). To get higher rates one needs higher power to drive the heater. To increase sensitivity in power readings for that sensor, one has to lower the gas pressure.

4. Discussions

4.1. Controlled high scanning rates

Linear heating and cooling at 130 000 K s^{-1} on Fig. 8 may appear unrealistically high. It is worth noting that the whole

heating and cooling cycle occurs within 1 ms. At this time scale the temperature of the membrane changes only at the vicinity of the heater. At 1 ms the heat capacity of addenda can be estimated as $<5 \times 10^{-9}$ J K^{-1} (N_2 contribution) plus $<4 \times 10^{-8}$ J K^{-1} (membrane contribution). Cooling power at 840 K was ~15 mW (as can be estimated from Fig. 10a), which makes a maximum cooling rate of >300 000 K s^{-1}. Fig. 10a shows the power released by the heater. At 5 ms ramp the addenda contribution is larger than in the experiment on Fig. 8; temperature swing was ~200 K at 40 000 K s^{-1} linear heating and cooling rates. At the lowest temperature (the most difficult region for fast cooling) the applied cooling power is approximately four times smaller than available cooling power, meaning that there is plenty of spare cooling power left.

The design of TCG-3880 sensor is not an optimum for high rate calorimetry: (i) the heater area is very small compared to the whole membrane, leading to the relatively large addenda contribution which lowers sensitivity; (ii) sample loading only on the area covered by the heater represents a technical challenge, misplacing the sample would create a significant temperature gradient across the sample and/or errors in sample temperature readings. In this respect microcalorimeter sensor design [5–7] is more advantageous. However TCG-3880 gives an example of how dramatically the response time of temperature sensing can be reduced by switching from two-component setup (heater and thermopile) to one-component setup (heater acting as a thermometer). In experiments on Fig. 5 there is a three orders of magnitude gain in a response time (from 5 ms for thermopile to <5 μs for the heater-thermometer). It is impossible to greatly improve thermopile response time by just moving hot junctions closer to the heater, at given sensor layout on microsecond time scale this thermopile would act more like an antenna picking up induced current from the heater, rather than a thermometer.

Schick's group used TCG-3880 sensor [10,11,28,29] and demonstrated a passive (not in real time) control of the rate which was made through adjusting a power on the heater by the "trial and error" method. Since the control was passive, actual scanning rate varied up to a factor of 3 during sample crystallization [10]. In addition, because sensor's thermopile was used as a thermometer, it resulted in 5 ms time resolution limit in isothermal experiments [28,29] and up to 50 K temperature resolution during scans (5 ms × 10 000 K s^{-1}). Temperature readings from the heater and active temperature control would alleviate these problems. Temperature readings from the heater alone (without active temperature control) would appreciably improve the system performance.

The introduction of an active control to the system may degrade the sensitivity of power measurements. As can be estimated from Fig. 4 in ref. [10], the resolution in heat flow determination in TCG-3880 with passive control was in the order of 4 μW (~30 nJ K^{-1} × 140 K s^{-1}). This is slightly better than 10 μW in the same sensor with active control. However, active control enables direct heat flow measurements, whereas passive control setup measures temperature difference and relies on calibration and models in heat flow determination [30].

4.2. Further improvements

The presented work proposes a new concept and provides an experimental prove of it based on hardware which was available to the author. There are a lot of possible improvements in the method. As for electronics, better optimized feedback control can be made: compensating for capacitance and inductance of wires to the sensor helps a lot to minimize transient response of the divider at short time scale; the divider itself can be made more linear e.g., by compensating the offset in U_{out}, seen in Fig. 5c, with part of U_{in} and by adjusting in real time the scaling factor U_0.

As for measuring cell, four-point resistance measurement of the heater is important. This cannot be done with TCG-3880 sensor. To minimize parasitic coupling, feeding and sensing leads of the membrane heater should be normal to each other. To minimize 'cold-edge' effect, another frame-like heater can surround the main heater and can shield radial heat flow. To increase sensitivity, relatively high underlying heat losses P_l and addenda contribution P_e can be compensated by differential setup (using reference membrane).

While it requires more complicated electronics, the sensing part of the proposed method is very simple, consisting of a single resistive element. Because of sensor's simplicity one can use multiple sensors in arrays similar to the layout for rapid thermal analysis [31]. One can scale the sensor size up for more robust setup with slower rates/larger samples.

5. Conclusion

The same resistive element, e.g., thin-film resistor, can be successfully used as a heater and as a temperature sensor in a setup with active temperature control. Based on that approach a micro-sized hot stage with high-speed temperature controller has been developed. The temperature controller has a microsecond time constant, which allows adjusting rapidly the power applied to the hot stage, depending on heat released/absorbed by a sample during an isotherm or during a given rate of temperature changes. The hot stage has low thermal inertia and, coupled with high-speed temperature controller, allows controlled cooling and heating rates up to 100 000 K s^{-1} and higher. The method can be a core of any setup where controlled fast temperature-time profile of thin or small sample is desirable. The proposed control circuit can be readily applied to the variety of the existing setups with resistive heater.

Acknowledgements

The author is grateful to Prof. Christoph Schick, University of Rostock, for providing with TCG-3880 sensors, and to Prof. Leslie H. Allen, University of Illinois at Urbana-Champaign, for providing with microcalorimeter sensors.

References

[1] V.B.F. Mathot, Thermochim. Acta 355 (2000) 1–33.
[2] B. Wunderlich, Thermochim. Acta 355 (2000) 43–57.

[3] T.F.J. Pijpers, V.B.F. Mathot, B. Goderis, R.L. Scherrenberg, E.W. van der Vegte, Macromolecules 35 (2002) 3601–3613.
[4] B. Fröchte, Y. Khan, E. Kneller, Rev. Sci. Instrum. 61 (1990) 1954–1957.
[5] S.L. Lai, G. Ramanath, L.H. Allen, P. Infante, Z. Ma, Appl. Phys. Lett. 67 (1995) 1229–1231.
[6] M.Y. Efremov, E.A. Olson, M. Zhang, Z. Zhang, L.H. Allen, Macromolecules 37 (2004) 4607–4616.
[7] M.Y. Efremov, E.A. Olson, M. Zhang, F. Schiettekatte, Z. Zhang, L.H. Allen, Rev. Sci. Instrum. 75 (2004) 179–191.
[8] V.M. Glazov, Yu.V. Yatmanov, Zhurnal Fizicheskoi Khimii 56 (1982) 755–760 (in Russian).
[9] E. Mayer, J. Appl. Phys. 58 (1985) 663–667.
[10] S.A. Adamovsky, A.A. Minakov, C. Schick, Thermochim. Acta 403 (2003) 55–63.
[11] A.A. Minakov, D.A. Mordvintsev, C. Schick, Polymer 45 (2004) 3755–3763.
[12] Y. Kraftmakher, Physics Reports 356 (2002) 1–117.
[13] A.W. van Herwaarden, P.M. Sarro, J.W. Gardner, P. Bataillard, Sens. Actuators A 43 (1994) 24–30.
[14] D.W. Denlinger, E.N. Abarra, K. Allen, P.W. Rooney, M.T. Messer, S.K. Watson, F. Hellman, Rev. Sci. Instrum. 65 (1994) 946–959.
[15] O. Riou, P. Gandit, M. Charalambous, J. Chaussy, Rev. Sci. Instrum. 64 (1997) 1501–1509.
[16] R.E. Cavicchi, G.E. Poirier, J.S. Suehle, M. Gaitan, N.H. Tea, US Patent #6,079,783, 27 June 2000.
[17] J. Lerchner, A. Wolf, G. Wolf, J. Therm. Anal. Calorimet. 57 (1999) 241–251.
[18] W. Winter, G.W.H. Höhne, Thermochim. Acta 403 (2003) 43–53.
[19] N.O. Birge, S.R. Nagel, Phys. Rev. Lett. 54 (1985) 2674–2677.
[20] D.G. Cahill, R.O. Pohl, Phys. Rev. B 35 (1987) 4067–4073.
[21] D.G. Cahill, M. Katiyar, J.R. Abelson, Phys. Rev. B 50 (1994) 6077–6081.
[22] D.M. Heap, M.G. Herrmann, C.T. Wittwer, Biotechniques 29 (2000) 1006–1012.
[23] A.I. Buzin, P. Kamasa, M. Pyda, B. Wunderlich, Thermochim. Acta 381 (2002) 9–18.
[24] See AD734 data sheet at http://www.analog.com.
[25] G.B. McKenna, private communications.
[26] See TCG-3880 datasheet at http://www.xensor.nl.
[27] M. Merzlyakov, Thermochim. Acta 403 (2003) 65–81.
[28] A.A. Minakov, D.A. Mordvintsev, C. Schick, Faraday Discuss. 128 (2004) 261–270.
[29] S.A. Adamovsky, C. Schick, Thermochim. Acta 415 (2004) 1–7.
[30] S.A. Adamovsky, private communications.
[31] J. Bennett, Proc. NATAS 2002 (2002) 150; US Patents #6,260,407; #6,265,226; #6,294,388; #6,477,479.